Supplementary Material Available. Tables of positional parameters, anisotropic thermal parameters, and a listing of F_o and F_c for the X-ray diffraction study of **3** were provided as supplementary information with the communication that reported part of the results discussed in this paper.[7] Ordering information is given on any current masthead page.

Registry No. 1, 12306-94-4; **2**, 12307-24-3; **3**, 106402-85-1; **3**-d_6, 118378-25-9; **4**, 118378-21-5; **5**, 118378-22-6; **6**, 118378-23-7; **7**, 41618-24-0; **8**, 118378-24-8; **9**, 80952-46-1; $CpRe(CO)_3$, 12079-73-1; $CpRe(CO)_2(PPh_3)$, 42766-75-6; $CH_3COCOCH_3$, 431-03-8; CH_3COCH_3, 67-64-1; $CpRe(CO)_2PMe_3$, 84521-32-4; $CpRe(CO)_2(COEt)Li$, 118378-26-0; $CH_3CH_2COCOCH_2CH_3$, 4437-51-8; $CH_3CH_2COCOCH_3$, 600-14-6; CCl_4, 56-23-5; $CBrCl_3$, 75-62-7; $CpRe(CO)_2H_2$, 80952-45-0; *trans*-$CpRe(CO)_2(CH_3)H$, 118455-81-5; $CpRe(CO)_2(CH_3)Cl$, 118378-27-1; CH_3COCl, 75-36-5; $CpRe(CO)_2Br_2$, 57194-43-1.

Synthesis, Characterization, and DNA-Binding Properties of (1,2-Diaminoethane)platinum(II) Complexes Linked to the DNA Intercalator Acridine Orange by Trimethylene and Hexamethylene Chains

Bruce E. Bowler,[1a] Kazi J. Ahmed,[1a] Wesley I. Sundquist,[1a] L. Steven Hollis,[1b] Edward E. Whang,[1a] and Stephen J. Lippard*,[1a]

Contribution from the Department of Chemistry, Massachusetts Institute of Technology, Cambridge, Massachusetts 02139. *Received June 16, 1988*

Abstract: We report the syntheses of intercalator-linked platinum complexes, $[Pt\{AO(CH_2)_n en\}Cl_2]Cl$, where $(CH_2)_n$ is a polymethylene chain having $n = 6$ (**9**) or $n = 3$ (**20**) linking the DNA intercalator acridine orange (AO) to the Pt-binding ligand ethylenediamine (en). Single-crystal X-ray diffraction studies of the oxalate (ox) derivative of **9**, $[Pt\{AO(CH_2)_6 en\}(ox)](NO_3)\cdot 7H_2O$ (**10**), and of the ligand precursors, $[AO(CH_2)_6OH]I$ (**5**) and $[AO(CH_2)_3OH]I$ (**15**), revealed the molecular structures and crystal packing of these compounds. In **10**, infinite "head-to-tail" stacking of the acridine orange rings occurs while the {Pt(en)(ox)} groups stack in a pairwise fashion. In compounds **5** and **15**, there are head-to-tail stacked acridine orange dimers with only weak interactions between the dimers. Visible absorption spectroscopy has been used to compare the effects of different chain lengths and substituents on the stacking interactions of these modified acridine orange compounds in solution. The tendency of molecules to aggregate in acidic aqueous solution follows the order $[Pt\{AO(CH_2)_3 en\}Cl_2]^+ \gg [Pt\{AO(CH_2)_6 en\}Cl_2]^+ > AO \gg [AO(CH_2)_6(en)]^+ > [AO(CH_2)_3(en)]^+$. The interaction of compounds **9** and **20** with DNA has also been studied by absorption spectroscopy. These results, together with the previously reported covalent binding to, and superhelical unwinding of, DNA by **9**, support a model in which the platinum moiety binds covalently to DNA while the AO moiety is intercalated one or two base pairs away.

We have recently been investigating the DNA-binding properties of organic intercalators and platinum complexes in the presence of one another. In part, our interest stems from the clinical success of the antitumor drug *cis*-diamminedichloroplatinum(II), *cis*-DDP,[2] which has stimulated much work on the interaction of platinum complexes with DNA, the proposed site of platinum antitumor activity.[3,4] Most chemotherapy protocols use *cis*-DDP in combination with one or more intercalative drugs, such as actinomycin,[5] and we wondered whether simultaneous binding of these two different classes of drugs might affect their individual interactions with DNA. Previously, we found that, at high drug-to-nucleotide ratios, the intercalator ethidium bromide can alter the mode and position of platinum binding to DNA.[6-8] These and studies by others[9] revealed that ethidium bromide can modulate *cis*-DDP binding to its preferred d(GpG) sites on DNA.

An important facet of this work has been the design and synthesis of a new class of bifunctional molecules comprised of the DNA intercalator acridine orange (AO) linked to the platinum

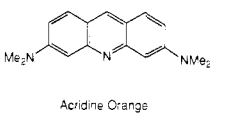

Acridine Orange

AO

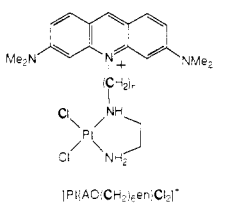

$[Pt\{AO(CH_2)_6 en\}Cl_2]^+$

complex, $[Pt(en)Cl_2]$, by trimethylene and hexamethylene chains. The acridine orange moiety binds to DNA in a reversible noncovalent intercalative fashion,[10] whereas the $[Pt(en)Cl_2]$ fragment binds covalently and essentially irreversibly to DNA. There is considerable precedent for combining several such functionalities into a single molecule in order to probe DNA sequence and structure. DNA footprinting and affinity cleaving agents,[11] metallointercalator DNA structure probes,[12] intercalator-linked oligonucleotides,[13] metallointercalator-modified DNA-binding

(1) (a) Massachusetts Institute of Technology. (b) Engelhard Corp.
(2) Hacker, M. P., Douple, E. B., Krakoff, I. H., Eds. *Platinum Coordination Compounds in Cancer Chemotherapy*; Nijhoff: Boston, 1984.
(3) Sherman, S. E.; Lippard, S. J. *Chem. Rev.* **1987**, *87*, 1153-1181.
(4) (a) Reedijk, J. *Pure Appl. Chem.* **1987**, *59*, 181-192. (b) Lippard, S. J. *Pure Appl. Chem.* **1987**, *59*, 731-742.
(5) Loehrer, P. J.; Einhorn, L. H. *Ann. Intern. Med.* **1984**, *100*, 704-713.
(6) Merkel, C. M.; Lippard, S. J. *Cold Spring Harbor Symp. Quant. Biol.* **1982**, *47*, 355-360.
(7) Tullius, T. D.; Lippard, S. J. *Proc. Natl. Acad. Sci. U.S.A.* **1982**, *79*, 3489-3492.
(8) Bowler, B. E.; Lippard, S. J. *Biochemistry* **1986**, *25*, 3031-3038.
(9) Malinge, J.-M.; Schwartz, A.; Leng, M. *Nucleic Acids Res.* **1987**, *15*, 1779-1797.
(10) Berman, H. M.; Young, P. R. *Annu. Rev. Biophys. Bioeng.* **1981**, *10*, 87-114.
(11) Dervan, P. B. *Science* **1986**, *232*, 464-471.
(12) Barton, J. K. *Science* **1986**, *233*, 727-734.

0002-7863/89/1511-1299$01.50/0

proteins,[14] and the many bis- and trisintercalators[15-20] all employ this concept.

The strategy used in the current work was to link the platinum and acridine functionalities in such a way that each could interact freely with DNA while being close enough to experience the structural perturbations of one another on the duplex. The compound [Pt{AO(CH_2)$_6$en}Cl_2]Cl (**9**) fulfills these requirements. When extended, its hexamethylene linker chain allows relatively independent motion of the AO and Pt constituents, and models revealed that when the platinum moiety is bound covalently to DNA, the AO ring can intercalate between base pairs adjacent to, or one removed from, the site of platination. The more constrained molecule, [Pt{AO(CH_2)$_3$en}Cl_2]Cl (**20**), in which the AO ring and the platinum complex are ~3.5 Å closer together, was synthesized to evaluate the effects of shortening the chain length.

In the present report, we present full details of the synthesis and characterization of [Pt{AO(CH_2)$_6$en}Cl_2]Cl (**9**) and [Pt{AO(CH_2)$_3$en}Cl_2]Cl (**20**), as well as the single-crystal X-ray structure determinations of the oxalate derivative, [Pt{AO(CH_2)$_6$en}(ox)](NO_3)·7H_2O (**10**) and the ligand precursors, [AO(CH_2)$_6$OH]I (**5**) and [AO(CH_2)$_3$OH]I (**15**). The effect of varying the side-chain length and substituents on self-association of these complexes in solution and the DNA-binding properties of these molecules has also been studied. A preliminary account of part of this work was reported previously.[21]

Experimental Section

Chemicals. Acridine orange from Aldrich was purified by a literature procedure.[22] 6-Chlorohexanol, 3-chlorohexanol, and dihydropyran from Aldrich were used without further purification. Silver iodide (Alfa) and oxalic acid (Mallinckrodt) were also used without further purification. Ethylenediamine (Mallinckrodt) was dried and distilled prior to use. Pyridinium *p*-toluenesulfonate (PPTS) was prepared by first hydrolyzing tosyl chloride in a 1:1 ethanol/water mixture and then generating the product from *p*-toluenesulfonic acid, as previously described.[23] The product was recrystallized from acetone. K_2PtCl_4 was obtained from Engelhard Corp. All other chemicals were reagent grade.

Buffers and DNA. CACE buffer was 10 mM sodium cacodylate, pH 7.0, and 1.0 mM Na_2EDTA. TE buffer was 10 mM Tris-HCl, pH 8.0, and 0.5 mM Na_2EDTA. Water used in the preparation of buffers was deionized with a system provided by Continental Water Systems. Calf thymus DNA used in absorption spectroscopic binding studies of Pt compounds was purified by extraction with phenol followed by dialysis against TE buffer. DNA concentrations were determined spectrophotometrically with the extinction coefficient ϵ_{260} = 6600 M^{-1} cm^{-1}.

Instrumentation and Analytical Methods. ^1H NMR spectra were obtained by using Bruker WM-250, Bruker WM-270, or Varian XL-300 NMR spectrometers. DMSO-d_6 and $CDCl_3$ were used as solvents, and ^1H NMR spectra were referenced to the residual solvent proton peak. DMSO samples were prepared in a drybox to exclude water. ^1H NMR chemical shifts in ppm for all compounds are reported with each synthetic procedure. ^{13}C NMR spectra were obtained in $CDCl_3$, DMSO-d_6, or D_2O with either a Bruker WM-270 (67.9 MHz), a JEOL FX90Q (22.6 MHz), or a Varian XL-300 (75 MHz) spectrometer. ^{13}C NMR chemical shifts in ppm are reported with each synthetic protocol and are referenced to the solvent peak or to dioxane (66.5 ppm) in the case of D_2O. ^{195}Pt NMR spectra were obtained on a Bruker WM-250 (53.8 MHz) or a Varian XL-400 (85.8 MHz) NMR spectrometer. Chemical shifts are reported in ppm relative to an aqueous solution of K_2PtCl_6 (0 ppm). Mass spectra were obtained in the laboratory of Professor K. Biemann at MIT under the direction of Dr. C. Costello, using the fast atom bombardment technique (FABMS). Glycerol (G) or dithiothreitol/dithioerthritol (DDT/DTE) matrices were used. Elemental analyses were performed by Atlantic Microlab or Galbraith Laboratories. Platinum analysis was done by atomic absorption spectroscopy using a Varian AA-1475 spectrometer equipped with a CRA-90 carbon rod atomizer.

Scheme I. Synthesis of Intercalator-Linked Alkyldiamine Ligands[a]

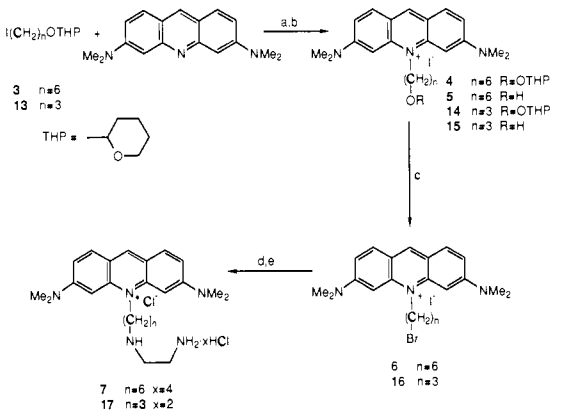

[a](a) Xylene, $NaHCO_3$ reflux. (b) 0.1 M HCl/ethanol, reflux. (c) 48% HBr, N_2, 95 °C. (d) 20-fold excess ethylenediamine, CH_3OH, N_2, reflux. (e) Ethanol, HCl(g).

Scheme II. Platination of Intercalator-Linked Alkyldiamine Ligands[a]

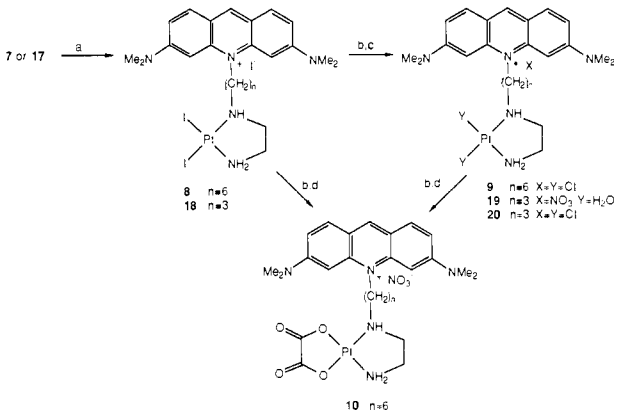

[a](a) K_2PtI_4, H_2O/DMF. (b) $AgNO_3$, DMF. (c) 1:10.4 M HCl/DMF. (d) Oxalic acid, H_2O.

Preparation of Compounds. Schemes I and II show the chemical route to the intercalator-linked compounds. Details of the synthesis of the ligands and their precursors, together with full spectroscopic and analytical data, may be found in the supplementary material.

[10-[6-[(2-Aminoethyl)amino]hexyl]-3,6-bis(dimethylamino)-acridinio]diiodoplatinum(II) Iodide (8). A solution of 0.5 g (0.85 mmol) of **7** was prepared initially in 10 mL of distilled H_2O, and the pH was adjusted to 10 with 1 M KOH. The solution was concentrated by rotary evaporation after adding 5 mL of DMF. A white solid (KCl) was removed by filtration, and the solution was diluted to 15 mL with 2:1 DMF/H_2O. A 0.5-g (1.2-mmol) portion of K_2PtCl_4 was dissolved in 5 mL of distilled H_2O, and 1.61 g of KI (9.69 mmol) was dissolved in 5 mL of distilled H_2O. The KI solution was added dropwise to the K_2PtCl_4 solution over 25 min, after which time the solution was heated at 50 °C for 15 min to form K_2PtI_4. Then 20 mL of DMF was added. The ligand solution was added slowly to the K_2PtI_4 solution over a 2-h period. DMF was added when needed to keep everything in solution. The solution was stirred overnight at 50 °C, the solvent reduced to a low volume by rotary evaporation, and distilled H_2O added to precipitate the product. This product was filtered, washed with EtOH and Et_2O, and then dried in a vacuum desiccator overnight, yielding 744.7 mg (89.2%) of **8** as bright orange powder. ^{195}Pt NMR (53.8 MHz, DMF): δ −3453.

[10-[6-[(2-Aminoethyl)amino]hexyl]-3,6-bis(dimethylamino)-acridinio]dichloroplatinum(II) Chloride, [Pt{AO(CH_2)$_6$en}Cl_2]Cl (9). A 300-mg (0.305-mmol) portion of **8** was dissolved in 15 mL of DMF. An

(13) Lancelot, G.; Asseline, U.; Thuong, N. T.; Hélène, C. *J. Biomol. Struct. Dyn.* **1986**, *3*, 913-921.
(14) Chen, C.-H. B.; Sigman, D. S. *Science* **1987**, *237*, 1197-1201.
(15) Ikeda, R. A.; Dervan, P. B. *J. Am. Chem. Soc.* **1982**, *104*, 296-297 and references therein.
(16) Gaugain, B.; Barbet, J.; Oberlin, R.; Roques, B. P.; Le Pecq, J.-B. *Biochemistry* **1978**, *17*, 5071-5078.
(17) Lown, J. W.; Gunn, B. C.; Chang, R.-Y.; Majundar, K. C.; Lee, J. S. *Can. J. Biochem.* **1978**, *56*, 1006-1015.
(18) Hansen, J. B.; Koch, T.; Buchardt, O.; Nielsen, P. E.; Nordén, B.; Wirth, M. *J. Chem. Soc., Chem. Commun.* **1984**, 509-511.
(19) Hansen, J. B.; Koch, T.; Buchardt, O.; Nielsen, P. E.; Wirth, M.; Nordén, B. *Biochemistry* **1983**, *22*, 4878-4886.
(20) Helbecque, N.; Bernier, J.-L.; Hénichart, J.-P. *Biochem. J.* **1985**, *225*, 829-832.
(21) Bowler, B. E.; Hollis, L. S.; Lippard, S. J. *J. Am. Chem. Soc.* **1984**, *106*, 6102-6104.
(22) Gupta, V. S.; Kraft, S. C.; Samuelson, J. S. *J. Chromatogr.* **1967**, *26*, 158-163.
(23) Miyashita, N.; Yoshikoshi, A.; Grieco, P. A. *J. Org. Chem.* **1977**, *42*, 3772-3774.

$AgNO_3$ solution containing 153.7 mg (0.905 mmol) of $AgNO_3$ dissolved in 3 mL of DMF was added dropwise to a solution of **8**. A heavy precipitate formed. The solution was heated on a steam bath to coagulate the AgI and then stirred for 5 min. The solution was filtered through a millipore filter (yield 203.8 mg, 95.9% of AgI), stirred for an additional 1 h, covered with foil, and then cooled in a refrigerator at 0 °C for 1 h. After it was again filtered through a millipore filter, the solution was concentrated by rotary evaporation to low volume, and 5 mL of DMF and 5 mL of 0.4 M HCl were added. After it stood overnight, the solution was filtered and reduced to a volume of 1–2 mL by rotary evaporation, and the product was precipitated by adding isopropyl alcohol. The solid was collected by suction filtration, washed with EtOH and Et_2O, and dried under an N_2 atmosphere. After the filtrate was dried in a vacuum desiccator, 196.3 mg of **9** (90.6%) was obtained as a bright red solid. Occasionally, **9** was contaminated with a water-insoluble impurity, which could be removed by dissolving **9** in water, filtering away the insoluble material, and isolating **9** from an aqueous HCl/DMF mixture by concentration and precipitation with *i*-PrOH. ^{13}C NMR (67.9 MHz, of diaqua derivative generated by adding 2.97 equiv of $AgNO_3$ to **9**, filtering the AgCl, and adjusting to pH 1 in D_2O, 318 K): δ 154.6 (2 C), 140.89, 140.76 (2 C), 132.1 (2 C), 115.4 (2 C), 113.3 (2 C), 90.6 (br, 2 C), 55.7, 53.2, 46.95, 46.86, 39.5 (4 C), 26.5, 25.8, 25.5, 24.8. ^{13}C NMR (67.9 MHz, of dichloro derivative in 2:1 D_2O–0.1 M HCl/DMF, 318 K): δ 155.2 (2 C), 142.0, 141.7 (2 C), 132.8 (2 C), 116.2 (2 C), 113.9 (2 C), 91.4 (2 C), 55.5, 52.5, 47.2, 46.8, 39.9 (4 C), 26.5, 25.8, 25.6, 25.2. ^{195}Pt NMR (in 2:1 0.1 M HCl/DMF): δ −2374. FABMS (G): *m/e* 766, $[M + G]^+$; 674, $[M]^+$; 660, $[M - CH_3 + H]^+$; 639, $[M - Cl]^+$; 408, $[M - PtCl_2]^+$; 266, $[M - C_8H_{19}N_2PtCl_2 + H]^+$. Anal. Calcd for $C_{25}H_{38}N_5Cl_3Pt$: C, 42.29; H, 5.39; N, 9.86; Cl, 14.98; Pt, 27.48. Found: C, 41.54; H, 5.48; N, 9.87; Cl, 15.03; Pt (by difference), 28.08.

[10-[6-[(2-Aminoethyl)amino]hexyl]-3,6-bis(dimethylamino)acridinio]oxolatoplatinum(II) Nitrate Dihydrate, [Pt{AO(CH$_2$)$_6$en}(ox)](NO$_3$)·2H$_2$O. A 984.5-mg (1.0-mmol) portion of **8** was dissolved in 40 mL of DMF. An $AgNO_3$ solution containing 526.7 mg (3.1 mmol) of $AgNO_3$ dissolved in 5 mL of DMF was added dropwise to the solution of **8**. The reaction was allowed to proceed in the dark for 16 h, and the precipitate, AgI, was removed by centrifugation. The product was precipitated from solution by addition of 300 mL of Et_2O, washed three times with Et_2O, collected by suction filtration, and washed further with Et_2O. The brick red solid (627 mg) was dried under vacuum over P_2O_5. A 70-mg portion of this solid was dissolved in 1.5 mL of H_2O and any insoluble material removed by centrifugation. The concentration of the acridine orange complex, 24.6 mM (73.7 μmol), was determined spectrophotometrically by using the measured extinction coefficient of **9** (ϵ_{473} = 4.48 × 10^4 M^{-1} cm^{-1}) as an approximation. This solution was added to 1.5 mL of a 100 mM solution of oxalic acid. The reaction was allowed to proceed for 12 h, and the product formed bright red crystals, which were collected by suction filtration and washed with ice-cold H_2O. The complex (**10**) is a heptahydrate, as revealed by X-ray crystallography. The crystals were crushed and dried for 3 days under vacuum over P_2O_5 but, nevertheless, analyzed for the presence of two water molecules. The yield for this step was 41.6 mg (overall yield 47.2%). Compound **10** can also be synthesized by an analogous procedure starting with [Pt{AO(CH$_2$)$_6$en}Cl$_2$]Cl (**9**) rather than the iodide derivative. ^{195}Pt NMR (in DMF): δ −2054. Anal. Calcd for $C_{27}H_{42}N_6O_9Pt$: C, 41.06; H, 5.36; N, 10.64. Found: C, 41.24; H, 5.08; N, 10.70.

[10-[3-[(2-Aminoethyl)amino]propyl]-3,6-bis(dimethylamino)acridinio]diiodoplatinum(II) Iodide, [Pt{AO(CH$_2$)$_3$en}I$_2$]I (18). K_2PtCl_4 (437 mg, 1.05 mmol) was dissolved in 12 mL of distilled H_2O. A KI solution (1.06 g, 6.39 mmol in 12 mL of distilled H_2O) was added dropwise to the K_2PtCl_4 solution. This mixture was then stirred at 50 °C for 20 min. A 500-mg (1.05-mmol) portion of **17** was dissolved in 60 mL of distilled H_2O, and the pH was adjusted to 10 with 1 M KOH. A total of 23 mL of DMF was added, and the solution was concentrated to remove most of the H_2O. Another 23 mL of DMF and 3 mL of distilled H_2O were added to redissolve the ligand. The K_2PtI_4 solution was added dropwise to the ligand. During the addition, 150 mL of DMF was added to the reaction mixture. The reaction solution was then stirred overnight at 60 °C. A white precipitate (KCl) was then filtered from the solution and the reaction mixture concentrated by rotary evaporation to low volume. A total of 200 mL of distilled H_2O was added, and the mixture was cooled to 0 °C for several hours. The precipitate was collected by suction filtration, washed with EtOH and Et_2O, and dried under vacuum, yielding 0.87 g (88%) of **18** as an orange powder. Anal. Calcd for $C_{22}H_{32}N_5I_3Pt$: C, 28.04; H, 3.42; N, 7.43. Found: C, 28.41; H, 3.44; N, 7.30.

[10-[3-[(2-Aminoethyl)amino]propyl]-3,6-bis(dimethylamino)acridinio]diaquaplatinum(II) Nitrate, [Pt{AO(CH$_2$)$_3$en}(H$_2$O)$_2$](NO$_3$)$_3$ (19). A 1.0-g (1.06-mmol) portion of **18** was suspended in 80 mL of DMF. An $AgNO_3$ solution prepared from 0.54 g (3.18 mmol) of $AgNO_3$ dissolved in 10 mL of DMF was added to the suspension of **18** and the mixture stirred in the dark for 3 days at 40 °C. AgI was removed by centrifugation. The DMF was removed by rotary evaporation. The solid was dissolved in distilled H_2O and dried again by rotary evaporation, yielding 0.8 g (96%) of **19**. Final purification was accomplished by anion exchange chromatography through Dowex 2-X8 (50–100 mesh) in the nitrate form. ^{13}C NMR (67.9 MHz, D_2O/DMF): 155.2 (br, 2 C), 141.5 (br), 141.4 (br, 2 C), 132.5 (br, 2 C), 115.9 (br, 2 C), 113.6 (br, 2 C), 91.1 (br, 2 C), 55.8 (br), 50.2 (br), 46.8 (br), 43.4 (br), 39.7 (br, 4 C), 23.0 (br). Anal. Calcd for $C_{22}H_{36}N_8O_{11}Pt$: C, 33.72; H, 4.63; N, 14.30. Found: C, 33.66; H, 4.43; N, 14.14.

[10-[3-[(2-Aminoethyl)amino]propyl]-3,6-bis(dimethylamino)acridinio]dichloroplatinum(II) Chloride Monohydrate, [Pt{AO(CH$_2$)$_3$en}Cl$_2$]Cl·H$_2$O (20). Compound **19** (250 mg, 0.32 mmol) was dissolved in 20 mL of DMF with heating on a steam bath. This solution was poured into 80 mL of 0.5 M HCl and cooled at 0 °C overnight. The precipitate was collected by centrifugation, washed with Et_2O, and dried under vacuum, yielding 162.3 mg (65%) of crude **20**. The crude product was dissolved in 1:1 EtOH/H_2O. Centrifugation yielded a pale pink pellet. The supernatant was cloudy and was diluted with 1:1 EtOH/distilled H_2O and centrifuged again at 20 000 rpm in a Sorvall RC2-B centrifuge using an SS-34 rotor. The clear supernatant was saved, and the pellet was redissolved in boiling 1:1 EtOH/H_2O. This procedure of centrifugation followed by resuspension was repeated until all material dissolved in a clear supernatant. The combined supernatants were concentrated by rotary evaporation to 20 mL, followed by the addition of 2 mL of 1 M HCl. The solution was cooled, and the precipitate was collected by centrifugation and dried under vacuum. This solid was suspended in distilled water and then collected again by centrifugation. After the solution was dried, under vacuum, 40 mg (16%) of **20** were obtained. FABMS (DTE/DTT): *m/e* 750, $[M - Cl + DTT - H]^+$; 714, $[M - 2Cl + DTT - 2H]^+$; 632, $[M]^+$; 366, $[M - PtCl_2]^+$; 352, $[M - PtCl_2 - CH_3 + H]^+$; 266, $[M - C_5H_{13}N_2PtCl_2 + H]^+$. Anal. Calcd for $C_{22}H_{34}N_5OCl_3Pt$ (IR indicates presence of water): C, 38.52; H, 5.00; N, 10.21; Cl, 15.50. Found: C, 38.63; H, 4.93; N, 10.24; Cl, 15.63.

Table I. Experimental Details[a,b] of the X-ray Diffraction Studies of [AO(CH$_2$)$_6$OH]I (**5**), [Pt{AO(CH$_2$)$_6$en}(ox)](NO$_3$)·7H$_2$O (**10**), and [AO(CH$_2$)$_3$OH]I (**15**)

	5	**10**	**15**
formula	$C_{23}H_{32}N_3OI$	$C_{27}H_{52}N_6O_{14}Pt$	$C_{20}H_{26}N_3OI$
a, Å	17.133 (2)	13.549 (5)	10.532 (3)
b, Å	15.013 (1)	16.179 (7)	11.140 (3)
c, Å	18.159 (1)	8.999 (4)	10.316 (2)
α, deg		96.63 (6)	115.74 (2)
β, deg	104.18 (1)	96.61 (4)	93.23 (2)
γ, deg		74.15 (4)	64.12 (2)
V, Å^3	4528 (1)	1878 (3)	967 (1)
Z	8	2	2
fw, g mol^{-1}	493.43	875.52	451.35
space group (No.)	*C*2/*c* (No. 15)	$P\bar{1}$ (No. 2)	$P\bar{1}$ (No. 2)
T, °C	23	23	23
λ, Å	0.7107	0.7107	0.7107
ρ_{obsd}, g cm^{-3}		1.57 (2)[c]	1.55 (1)[c]
ρ_{calcd}, g cm^{-3}	1.447	1.548	1.549
μ, cm^{-1}	14.53	40.05	16.92
R_1[d]	0.0463	0.0471	0.0358
R_2[e]	0.0523	0.0563	0.0517

[a] Data were collected by $\theta/2\theta$ scans on an Enraf-Nonius CAD-4F κ-geometry diffractometer at 23 ± 1 °C. [b] For typical procedures, see: Silverman, L. D.; Dewan, J. C.; Giandomenico, C. M.; Lippard, S. J. *Inorg. Chem.* **1980**, *19*, 3379. [c] Measured by neutral buoyancy in aqueous CsCl. [d] $R_1 = \sum||F_o| - |F_c||/\sum|F_o|$. [e] $R_2 = [\sum w(|F_o| - |F_c|)^2/\sum w|F_o|^2]^{1/2}$.

Collection and Reduction of X-ray Data. [AO(CH$_2$)$_6$OH]I (5). A bright red needle of **5** of dimensions 0.14 × 0.10 × 0.16 mm was mounted with epoxy resin in a capillary tube. Open counter ω scans of low-angle reflections revealed structureless profiles, and the peak widths were judged to be acceptable ($\Delta\omega_{1/2}$ = 0.1°). Intensity data and unit cell parameters were measured as described in Table I. From the extinctions, the space group could be either *Cc* or *C*2/*c*.[24] Statistical analysis of the data suggested the centrosymmetric space group *C*2/*c*, and this choice was confirmed by successful refinement of the structure. Experimental

(24) Hahn, T., Ed. *International Tables for X-ray Crystallography*; Reidel: Dordrecht, The Netherlands, 1983; Vol. A, pp 102–105, 142–149, and 182–189.

details of the data collection and reduction are given in Table I.

[Pt{AO(CH$_2$)$_6$en}(ox)](NO$_3$)·7H$_2$O (10). Bright red, platelike crystals of **10** formed directly from aqueous solution in the reaction of oxalic acid with either **8** or **9**, following the removal of the halides by $AgNO_3$. A crystal of approximate dimensions 0.4 × 0.2 × 0.1 mm was sealed in a glass capillary next to a pool of mother liquor to prevent solvent loss, which occurs rapidly in air. The crystal quality was judged to be acceptable on the basis of open counter ω scans of several low-angle reflections ($\Delta\bar{\omega}_{1/2}$ = 0.19°). Study on the diffractometer revealed a triclinic system with space group either $P1$ or $P\bar{1}$.[24] Statistical analysis favored the centrosymmetric space group, and this choice was confirmed by successful refinement of the structure. Precession photographs using Cu K$\bar{\alpha}$ (λ 1.5418 Å) radiation were taken to confirm the space group and unit cell dimensions. Further experimental details of the X-ray diffraction study of **10** are given in Table I.

[AO(CH$_2$)$_3$OH]I (15). Crystals of compound **15** were grown by slow evaporation of a saturated solution in methanol. A bright red crystal of dimensions 0.7 × 0.3 × 0.2 mm was mounted with epoxy resin on the end of a glass fiber. Open counter ω scans of low-angle reflections revealed structureless profiles, and the peak widths were judged acceptable ($\Delta\bar{\omega}_{1/2}$ = 0.15°). Intensity data and unit cell parameters were measured as described in Table I. The space group could be either $P1$ or $P\bar{1}$.[24] Statistical analysis favored the centrosymmetric space group, and this choice was confirmed by successful refinement of the structure. Further experimental details of the X-ray diffraction study of **15** are given in Table I.

Structure Determination and Refinement. [AO(CH$_2$)$_6$OH]I (5). The iodide atom was located from a Patterson map. All remaining non-hydrogen atoms were found in subsequent difference Fourier maps. Neutral-atom scattering factors and anomalous dispersion corrections for non-hydrogen atoms were taken from ref 25. All hydrogen atoms were placed in their calculated positions, d(C–H) = 0.95 Å, and constrained to "ride" on the atoms to which they are attached, except for the methylene hydrogens on C20, which were omitted owing to disorder in the hydroxyl oxygen atom. The hydrogen atoms were assigned common isotropic thermal parameters as groups depending on whether they were bonded to a sp^2(H), sp^3(CH$_2$), or sp^3(CH$_3$) hybridized carbon atom. These thermal parameters converged to U = 0.067, 0.148, and 0.093 Å^2, respectively.

With use of SHELX-76,[26] full-matrix least-squares refinement was carried out. The oxygen atom was found to be disordered over two positions. Refinement went smoothly, assuming an equal population of the two positions and minimizing the function $\sum w(|F_o| - |F_c|)^2$, where $w = 1.3345/[\sigma^2(F_o) + 0.000625(F_o)^2]$. The largest peaks in the final difference Fourier map were located within 1.2 Å of the iodide atom. Further information is given in Table I.

Figure S1 displays the structure and labeling scheme of the cation and Figure S2 displays the intermolecular packing of the cation. Final non-hydrogen atom positional and thermal parameters, together with their estimated standard deviations, are reported in Table S1 and S2, respectively (supplementary material). Bond lengths and angles with their estimated standard deviations are summarized in Table S3. A listing of observed and calculated structure factors is given in Table S4 and hydrogen atom positional parameters in Table S5.

[Pt{AO(CH$_2$)$_6$en}(ox)](NO$_3$)·7H$_2$O (10). The position of the platinum atom was located from a Patterson map. All remaining non-hydrogen atoms were revealed in subsequent difference Fourier maps. The structure was refined with anisotropic thermal parameters for all non-hydrogen atoms except those of six of the water molecules. The orientation of the hydrogen atoms was determined from difference Fourier maps, and the hydrogens were constrained to ride on the atoms to which they are attached. Two of the eight water molecules located (O6W and O8W) had unacceptably large thermal parameters. These two water molecules were thus assigned thermal parameters of B = 20.0 and their occupancy factors refined to 0.568 and 0.482, respectively. These atoms were subsequently refined with fixed occupancy factors of 0.5. Allowing half-occupancy at these positions yields a calculated density in reasonable agreement with that observed (Table I). The largest peak in the difference map was 0.9 e Å^{-3} in the vicinity of solvent water molecules O6W and O8W.

Figure 1 displays the structure of the cation. Final atomic positional and thermal parameters are given in Tables S6 and S7, respectively (supplementary material). Interatomic distances and bond angles with their estimated standard deviations are given in Table S8. A listing of observed and calculated structure factors is supplied in Table S9.

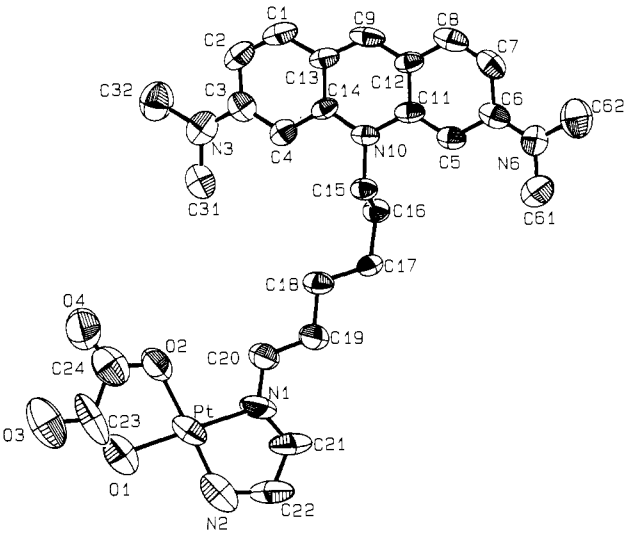

Figure 1. Structure of the [Pt{AO(CH$_2$)$_6$en}(ox)]$^+$ (**10**) cation, showing 40% probability thermal ellipsoids and atom-labeling scheme.

[AO(CH$_2$)$_3$OH]I (15). The position of the iodide atom was located from a Patterson map. All remaining non-hydrogen atoms were revealed in subsequent difference Fourier maps. The structure was refined with anisotropic thermal parameters for all non-hydrogen atoms. The hydrogen positions were located from difference Fourier maps and were constrained to ride on the atoms to which they are attached. The largest peak in the difference map was 0.85 Å from the iodide anion.

Figure S3 displays the structure of the cation and Figure S4 the intermolecular packing of the cation (supplementary material). Final atom positional and thermal parametrs are given in Tables S10 and S11, respectively. Interatomic distances and bond angles with their estimated standard deviations are given in Table S12. A listing of observed and calculated structure factors is supplied in Table S13.

Concentration Dependence of the Visible Absorption Spectra of Acridine Intercalators and the Determination of Monomer–Dimer Isosbestic Points. These measurements were carried out by the method of Lamm and Neville.[27] Individual dilutions were made from stock solutions by using deionized water in a polyethylene bottle. Final volumes were on the order of 9–12 mL. Each dilution was made just before measurement. The solution was mixed with gentle swirling and added to either a 0.1- or 1.0-cm-path-length quartz cuvette. Spectra were recorded on a Perkin-Elmer 330 or Lambda 7 spectrometer. Spectra were measured at six or more concentrations in the 10^{-4}–10^{-6} M range. Extinction coefficients were calculated at a series of wavelengths for each compound, and molar absorption (ϵ) versus wavelength (λ) was plotted for each concentration. The isosbestic points were determined from these plots. The ϵ_{ip} was taken as the average of the observed values for each concentration at that wavelength and the values obtained are reported below.

Solutions of **9**, **20**, and the corresponding unplatinated ligands, **7** and **17**, were prepared in approximately 100 μM concentrations before addition to DNA solutions (see below). Concentrations were determined spectrophotometrically by using the extinction coefficients of the monomer/dimer isosbestic points, ϵ_{ip}. The very low solubility of **20** precluded accurate measurement of its ϵ_{ip}, so the ϵ_{ip} of **9** was used as an approximation. Platinum stock solutions were prepared as previously described, and concentrations were determined spectrophotometrically.[8]

Visible Absorption Studies of Intercalator Binding to DNA. A solution was prepared containing 10 mM Tris-HCl (pH 8.0), 0.2 mM Na_2EDTA, 120 μM calf thymus DNA, and 4.8 μM **9** at a drug-to-nucleotide (D/N) ratio of 0.04. This mixture was covered with foil to protect it from light exposure and incubated for 25 h at 37 °C in a water bath. The mixture was then concentrated from 9.3 to 0.8 mL and divided in half and ethanol-precipitated as before.[8] One of the two DNA/**9** pellets was resuspended in 1 mL of CACE buffer. The visible absorption spectrum was recorded in the range 640–360 nm. This solution was then diluted 1 in 10 and the bound platinum and DNA concentrations were determined as described above, yielding [Pt{AO(CH$_2$)$_6$en}Cl$_2$]Cl = 13.5 μM and [DNA-P$_i$] = 431 μM, for a (D/N)$_b$ = 0.031.

Solutions of **9** and **20** with DNA were prepared in 1-mL volumes of deionized water that were 10 mM in sodium cacodylate, 6.6 mM in

(25) *International Tables for X-ray Crystallography*; Ibers, J. A., Hamilton, W. C., Eds.; Kynoch: Birmingham, England, 1974; Vol. IV, pp 99 and 149.

(26) Sheldrick, G. M. In *Computing in Crystallography*; Schenck, H., Olthof-Hazenkamp, R., van Koningsveld, H., Bassi, G. C., Eds.; Delft University Press: Delft, The Netherlands, 1978; pp 34–42.

(27) Lamm, M. E.; Neville, D. M., Jr. *J. Phys. Chem.* **1965**, *69*, 3872–3877.

Tris-HCl, and 1.65 mM in Na_2EDTA (pH 7.2) and were 431 μM in calf thymus DNA and 13.5 μM in intercalator. Solutions without DNA were also prepared for each intercalator as controls. All spectra were recorded as described above in 1-cm-path-length quartz cuvettes, immediately after preparation, against a blank cell containing only buffer. Spectra were manipulated and stored with a Perkin-Elmer 3600 data station. The **9**/DNA and **20**/DNA solutions were then incubated at 37 °C for 48 h in the dark. The Eppendorf tubes containing these solutions were sealed with Teflon tape to minimize solvent loss owing to evaporation, and the solution volumes were carefully measured before and after incubation to ensure that no significant volume changes occurred. The visible spectra were then remeasured.

Results and Discussion

Synthetic Strategy. In designing the synthesis of a DNA-binding intercalator-linked platinum complex, several considerations were important. We desired a readily available intercalator, which could be easily functionalized without requiring lengthy synthesis from constituent fragments of the aromatic system. A well-characterized DNA intercalator was also an important consideration. Acridines were an ideal choice, since many varieties are commercially available, and the intact ring system is easily functionalized with side chains at either the C9[28] or N10[29] ring positions. Acridine orange was selected because it is one of the best characterized acridine intercalators and synthetically it can be quarternized at the N10 atom without concern for reaction at the dimethylamino substituents.[29] Quarternization at N10, as opposed to functionalization of C9, was preferred because the crystal structure of acridine orange, intercalated into a self-complementary d(CpG) sequence, clearly shows that N10 projects into the major groove of the DNA.[30] Platinum complexes bind selectively to N7 atoms of guanine in the major groove. Thus, molecules **9** and **20** were chosen as initial synthetic targets because they contain two linked DNA-binding moieties capable of reacting independently in the major groove of the double helix. By varying the chain length, the effect of platinum acridine orange proximity on the DNA-binding properties of the compounds could be investigated.

Synthesis of Acridine Orange Linked Alkyldiamine Ligands. The syntheses of **7** and **17** are outlined in Scheme I. The starting materials for N10 quarternizing agents were 6-chlorohydroxyhexane and 3-chlorohydroxypropane. The hydroxy groups of these compounds were first protected as tetrahydropyranyl ethers through treatment with dihydropyran in the presence of PPTS as a catalyst.[23] The chloro substituents of **2** and **12** were then converted to iodo groups by a Finkelstein reaction,[31] yielding compounds **3** and **13**, respectively. These compounds were used to quarternize the N10 atom of AO by refluxing a 2-fold excess of **3** or **13** with AO in xylene.[32-34] A trace of $NaHCO_3$ was added to prevent deprotection of the hydroxy substituent. Analogous reaction of AO with the chlorohydrins **1** and **11** resulted in no quaternization of the N10 atoms.

Deprotection of the hydroxy substituents of **4** and **14** was accomplished by refluxing in acidic ethanol.[35] Compound **5** was recrystallized from isopropyl alcohol/methanol, yielding deep red needles, which were characterized by X-ray crystallography. Compound **15** proved to be considerably less soluble than **5** in alcohols and thus recrystallization required large volumes of methanol. The resulting bright red needles were also characterized by X-ray crystallography. Analytical and crystallographic data demonstrate that solids **5** and **15** are iodide salts, despite the presence of excess HCl. The trimethylene-quarternized acridine orange compounds are considerably less soluble than their hexamethylene counterparts in any given solvent. Treatment of **5** and **15** with 48% HBr[36] at 95 °C produced the bromo derivatives **6** and **16**, respectively. Analytical data (supplementary material) indicate that iodide persisted as counterion in these compounds as well, despite the presence of excess bromide, presumably because the iodide salts are less soluble.

Ligands **7** and **17** were synthesized by displacement of bromide by ethylenediamine.[16] The solvent must be dry so as to prevent hydroxide substitution of bromide, and a large excess of ethylenediamine was required to prevent formation of multiply substituted ethylenediamines. The excess ethylenediamine was easily removed by rotary evaporation in the presence of DMF. The crude ligands were purified by recrystallization from ethanol (methanol for **17**) through which dry HCl gas was bubbled. For **7**, it is important that the ethanol be dry since otherwise only oils are obtained, whereas, for **17**, it is preferable that the methanol contain 1–2% water to aid in dissolving the crude product. Elemental analyses indicated that recrystallization of **7** yields the tetrahydrochloride salt, whereas recrystallization and anion exchange chromatography of **17** yields the dihydrochloride salt. Despite the low pK_a (−3.15) of the dimethylamino substituents of AO,[37] protonation seems to occur in dry HCl-saturated ethanol. Evidently, the presence of water during the recrystallization of **17** makes protonation of the dimethylamino substituents unfavorable.

The ^{13}C NMR spectra of **7** and **17** revealed the appearance of two peaks in the region expected for an asymmetrically alkylated ethylenediamine. Addition of ethylenediamine to a ^{13}C NMR sample of **7** caused the appearance of a new peak at 41.7 ppm, which was distinct from the peaks attributable to the ethylenediamine unit of $[AO(CH_2)_6(en)]Cl$.

Platination of Ligands 7 and 17. Ligands **7** and **17** could not be platinated by methods usually employed in aqueous solution,[38] since addition of $[PtI_4]^{2-}$ to **7** or **17** immediately precipitated an insoluble salt. We attempted to platinate the ligands with the neutral platinum reagents, *cis*-$[Pt(PhCN)_2Cl_2]$, $[Pt(COD)Cl_2]$ (COD = 1,5-cyclooctadiene), and *cis*-$[Pt(DMSO)_2Cl_2]$, all with poor results. Apparently, alkylamines react with platinum-bound PhCN[39] and COD.[40,41] In reactions with *cis*-$[Pt(DMSO)_2Cl_2]$, we were unsuccessful in removing DMSO from the final product by using literature procedures.[42,43]

Ultimately, platinum complexes of **7** and **17** were successfully obtained by a modification of Dhara's method[38] (Scheme II), employing DMF as solvent to prevent precipitation of **7** and **17** with $[PtI_4]^{2-}$. K_2PtI_4 was generated in aqueous solution from K_2PtCl_4, transferred to DMF, and allowed to react with **7** or **17** to produce **8** or **18**. Metathesis of the iodides proceeded smoothly in DMF by treating **8** with $AgNO_3$, producing the intermediate diaqua complex. The dichloro compound **9** was generated from the diaqua complex by adding aqueous HCl/DMF. The aqueous solubility of **9** exceeds 20 mg/mL. The oxalate derivative, **10**, formed crystals suitable for X-ray diffraction studies. This compound was prepared by $AgNO_3$ treatment of either **8** or **9** in DMF and addition of oxalic acid in H_2O. The resulting oxalate complex crystallizes as a nitrate salt from H_2O as it forms. The low solubility of **18** in DMF made it difficult to use the metathesis reaction employed for **8**. We therefore isolated the intermediate

(28) Adcock, B. In *Acridines*, 2nd ed.; Acheson, R. M., Ed.; Wiley-Interscience: New York, 1973; pp 109–140.
(29) Selby, I. A. In *Acridines*, 2nd ed.; Acheson, R. M., Ed.; Wiley-Interscience: New York, 1973; pp 433–517.
(30) Wang, A. H.-J.; Quigley, G. J.; Rich, A. *Nucleic Acids Res.* **1979**, *6*, 3879–3890.
(31) Buehler, C. A.; Pearson, D. E. *Survey of Organic Synthesis*; Wiley-Interscience: New York, 1970; p 339.
(32) Acheson, R. M.; Harvey, C. W. C. *J. Chem. Soc., Perkin Trans. 1* **1976**, 465–470.
(33) Miethke, E.; Zanker, V. *Z. Phys. Chem. (Munich)* **1958**, *18*, 375–390.
(34) Zanker, V.; Erhardt, E.; Mader, F.; Thies, J. *Z. Naturforsch.* **1966**, *21B*, 102–108.
(35) van Boom, J. H.; Herschied, J. D. M.; Reese, C. B. *Synthesis* **1973**, 169–170.
(36) Cortese, F. In *Organic Syntheses*; Blatt, A. H., Ed.; Wiley: New York, 1943; Collect. Vol. II, pp 91–93.
(37) Albert, A. *The Acridines: Their Preparation, Physical, Chemical and Biological Properties*, 2nd ed.; Edward Arnold: London, 1966.
(38) Dhara, S. C. *Ind. J. Chem.* **1970**, *8*, 193–194.
(39) Stephenson, N. C. *J. Inorg. Nucl. Chem.* **1962**, *24*, 801–808.
(40) Paiaro, G.; De Renzi, A.; Palumbo, R. *J. Chem. Soc., Chem. Commun.* **1967**, 1150–1151.
(41) Palumbo, R.; De Renzi, A.; Panunzi, A.; Paiaro, G. *J. Am. Chem. Soc.* **1969**, *91*, 3874–3879.
(42) Romeo, R.; Minniti, D.; Lanza, S.; Tobe, M. L. *Inorg. Chim. Acta* **1977**, *22*, 87–91.
(43) Tobe, M. L.; Schwab, A. P.; Romeo, R. *Inorg. Chem.* **1982**, *21*, 1185–1190.

diaqua complex **19** and purified it by anion exchange chromatography. Contamination of **20** with AgCl was still a problem and, because of the low aqueous solubility of **20** (upper limit ~0.15 mM), the AgCl had to be removed by a lengthy centrifugation procedure. The overall yield of the nine-step sequence used to prepare the intercalator-linked platinum complexes, based on acridine orange, was 31.3% for **9** and only 3.4% for **20**.

^{13}C NMR spectroscopy provided definitive evidence for platinum binding to the ethylenediamine moiety of **9** and **20**. The three carbons attached to the ethylenediamine nitrogen atoms all showed downfield shifts of 6–11 ppm for platinum diaqua complexes versus the unbound ligands. This observation is consistent with the 6.8 ppm downfield shift seen for ethylenediamine (41.7 ppm) when bound to platinum, for example in $[Pt(en)(H_2O)_2]^{2+}$ (47.5 ppm).

^{195}Pt NMR spectroscopy is diagnostic of the coordination environment of platinum complexes. Compound **9** exhibited one resonance at δ −2374 (2:1 0.1 M HCl/DMF), which compares well with the resonance at δ −2379 (2:1 M HCl/DMF) observed for $[Pt(en)Cl_2]$. Compound **8** showed one resonance at δ −3453 (DMF), which is shifted significantly upfield from the dichloro complex. A shift of this magnitude is expected when chloride is replaced by iodide in the platinum coordination sphere.[44] Similar ^{195}Pt chemical shifts have been reported in DMF for $[Pt(en)I_2]$ (δ −3461) and a halide-bridged compound $[Pt_2(en)_2I_2]I_2$ (δ −3457).[45] Compound **10** showed a ^{195}Pt chemical shift of δ −2054.

Description of the Structures. Figure 1 displays the structure of the intercalator-linked cation, $[Pt\{AO(CH_2)_6en\}(ox)]^+$ (**10**). The X-ray structures of the synthetic intermediates, $[AO(CH_2)_6OH]I$ (**5**) and $[AO(CH_2)_3OH]I$ (**15**), have also been determined; they are given in Figures S1 and S3, respectively. The bond lengths and angles for the acridine orange ring in all three compounds are very similar to those reported in previous studies of acridine orange.[46-48] In particular, some bonds show essentially double-bond character (C1–C2 and C7–C8), whereas others have much more single-bond character (C2–C3, C6–C7, C1–C13, C8–C12, C3–C4, and C5–C6). Previous structural work on acridine orange revealed deviations from the usual 120° sp^2 bond angle near the protonated N10 atom, such that the angle C14–N10–C11 increased to 124.5–125.2°, while the angles C13–C14–N10 and N10–C11–C12 decreased to approximately 118°. Quarternization of the N10 atom in **5**, **10**, and **15** produces a similar effect; however, smaller increases in the C14–N10–C11 angle (123.4 (7)° in **5**, 122.9 (9)° in **10**, and 122.3 (2)° in **15**) are observed. Increases in the N10–C11 and N10–C14 bonds of about 0.2 Å relative to the same bonds in acridine orange are also found. These differences probably result from the N10 atom lone pair being involved in a bond to carbon versus a proton.[49] The quarternized AO rings in all three structures are nearly planar, with the dimethylamino groups both twisted slightly, the Me–N–C–C torsion angles ranging from 1.0–6.0°. Similar deviations from planarity occur for C9-substituted acridines[50] and may be a general phenomenon resulting from substitution on the central acridine ring. The alkyl side chains project below the acridines in extended conformations. Bond lengths and angles within the alkyl chains are typical of sp^3 carbon–carbon bonds except near the disordered alcohol oxygen position in **5**.

The coordination about platinum in **10** is approximately square planar with angular deviations due to the chelating oxalate and ethylenediamine ligands (O1–Pt–O2, 82.8 (5)°; N1–Pt–N2, 82.0 (5)°). The oxalate ligand is symmetrically coordinated to the platinum center (Pt–O1, 2.01 (1) Å; Pt–O2, 2.02 (1) Å); however, the ethylenediamine moiety is asymmetrically coordinated (Pt–N1, 2.02 (1) Å; Pt–N2, 1.92 (2) Å). The longer bond distance observed for the secondary amine is probably due to steric factors.

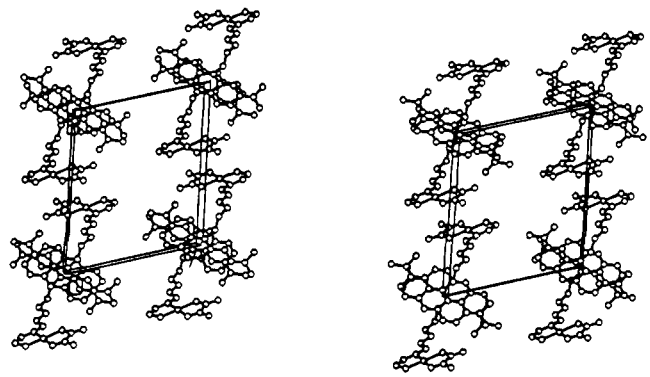

Figure 2. Stereoview of the unit cell of $[Pt\{AO(CH_2)_6en\}(ox)](NO_3)\cdot 7H_2O$ (**10**). The nitrate anions and water molecules are omitted for clarity. View is along the [001] axis.

Examination of crystal-packing stereoviews for **5** and **15** (Figures S2 and S4, respectively) reveals that in both cases the AO rings are stacked in a head-to-tail fashion, with the long axes of the AO rings parallel to each other. The acridine rings of **5** stack in pairs (3.5 Å) with the central and one outer ring overlapping completely, while the acridine rings of **15** are infinitely stacked (3.5 Å) with a similar two-ring overlap. In the crystal structure of a 9-aminoacridine derivative having a six-carbon alkylamino side chain, the rings are also stacked in pairs; however, the side chains project toward the other member of the pair so as to wrap around it.[50]

A stereoview of **10** (Figure 2) shows the acridine orange rings to be infinitely stacked in a head-to-tail fashion at a 38° angle with respect to the [001] direction. The average intermolecular ring distance is 3.5 Å, indicating strong π overlap. The {Pt(en)(ox)} units stack in a pairwise, head-to-tail fashion along [010]. The stacking distance between the planes is 3.6 Å; however, the units are offset, presumably to minimize the overlap of the oxalate rings, giving a Pt–Pt interatomic distance of 4.46 Å.

Eight water molecule positions per asymmetric unit were identified in the structure of **10**; two of which are only half-occupied. The water molecules form an extensive hydrogen-bonding network.

Spectroscopic Studies of Self-Association of Ligands 7 and 17 and Platinum Complexes 9 and 20. Acridine orange and other chromophores display effects of self-association in their electronic absorption spectra.[51] Absorption bands at ~492 and ~470 nm have been assigned to acridine orange monomers and stacked dimers, respectively.[27] The molar absorptivity (ϵ) versus wavelength (λ) was measured for various concentrations of $[AO(CH_2)_6(en)]Cl$ (**7**), $[Pt\{AO(CH_2)_6en\}Cl_2]Cl$ (**9**), and $[AO(CH_2)_3(en)]Cl$ (**17**). At low concentration (<20 μM), a peak at ≈495 nm dominates in the absorption spectrum of each compound. As the concentrations are raised, an absorption band near 470 nm becomes increasingly prominent. From the concentration dependence of the absorption spectra of these compounds, we derive the following extinction coefficients for the monomer/dimer isosbestic points: $[Pt\{AO(CH_2)_6en\}Cl_2]Cl$, $\epsilon_{473} = (4.48 \pm 0.04) \times 10^4$ M^{-1} cm^{-1}; $[AO(CH_2)_6(en)]Cl$, $\epsilon_{475} = (4.75 \pm 0.04) \times 10^4$ M^{-1} cm^{-1}; $[AO(CH_2)_3(en)]Cl$, $\epsilon_{480} = (4.5 \pm 0.1) \times 10^4$ M^{-1} cm^{-1}. The corresponding value for AO is $\epsilon_{470} = 4.3 \times 10^4$ M^{-1} cm^{-1}.[27] The shift in the isosbestic point to longer wavelength upon quarternization is paralleled by a shift in the maximum of the monomer band from 492 nm for AO to 495 nm for **9** and **7** and to 498 nm for **17**.[27]

The tendency of molecules to self-associate in solution follows the order $[Pt\{AO(CH_2)_3en\}Cl_2]Cl \gg [Pt\{AO(CH_2)_6en\}Cl_2]Cl >$ AO $\gg [AO(CH_2)_6(en)]Cl > [AO(CH_2)_3(en)]Cl$. The lesser

(44) Pregosin, P. S. *Coord. Chem. Rev.* **1982**, *44*, 247–291.
(45) O'Halloran, T. V.; Lippard, S. J.; Richmond, T. J.; Klug, A. *J. Mol. Biol.* **1987**, *194*, 705–712.
(46) Kuban, R.-J.; Kulpe, S.; Schulz, B. *Cryst. Res. Technol.* **1985**, *20*, 1073–1077.
(47) Mattia, C. A.; Mazzarella, L.; Vitagliano, V.; Puliti, R. *J. Crystallogr. Spectrosc. Res.* **1984**, *14*, 71–87.
(48) Obendorf, S. K.; Glusker, J. P.; Hansen, P. R.; Berman, H. M.; Carrell, H. L. *Bioinorganic Chem.* **1976**, *6*, 29–44.
(49) Singh, C. *Acta Crystallogr.* **1965**, *19*, 861–864.
(50) Glusker, J. P.; Gallen, B.; Carrell, H. L. *Acta Crystallogr.* **1973**, *B29*, 2000–2006.
(51) Porumb, H. *Prog. Biophys. Mol. Biol.* **1978**, *34*, 175–195.

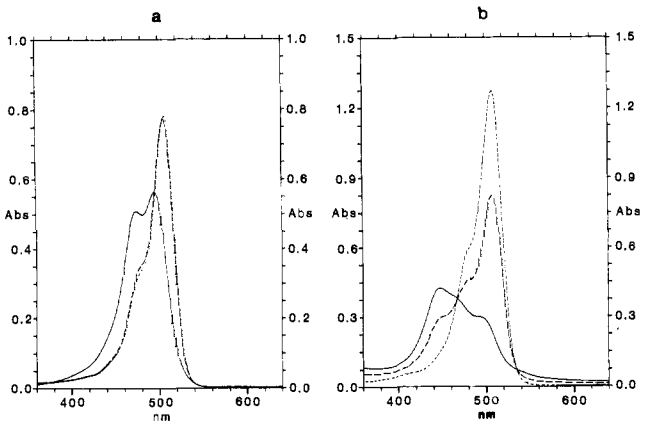

Figure 3. Visible absorption spectra of (a) $[Pt\{AO(CH_2)_6en\}Cl_2]Cl$ (**9**) and (b) $[Pt\{AO(CH_2)_3en\}Cl_2]Cl$ (**20**) in the absence (—) of DNA, immediately after addition to a DNA solution (– – –), and after a 48-h incubation (- - -) of the drug/DNA solution. The buffer in all samples is 10 mM sodium cacodylate, 6.6 mM Tris-HCl, 1.65 mM Na_2EDTA, pH 7.2. The calf thymus DNA phosphate concentration is 431 μM, and the concentration of the intercalator is ~13.5 μM, giving D/N = 0.031.

tendency of $[AO(CH_2)_6(en)]Cl$ and $[AO(CH_2)_3(en)]Cl$ to aggregate probably results from the hydrophilic protonated ethylenediamine unit, which would be expected to be more highly solvated. The greater proximity of the ethylenediamine unit to the hydrophobic ring may account for $[AO(CH_2)_3(en)]Cl$ having the lowest tendency to aggregate. Similarly, the presence of a poorly solvated $\{Pt(en)Cl_2\}$ unit may tend to enhance the aggregation of the $[Pt\{AO(CH_2)_6en\}Cl_2]Cl$ and $[Pt\{AO(CH_2)_3en\}Cl_2]Cl$ molecules relative to unsubstituted acridine orange. That the side chains do affect the stacking of these molecules is seen from differences in the solid-state structures of $[AO(CH_2)_6OH]I$ and $[Pt\{AO(CH_2)_6en\}(ox)](NO_3)\cdot 7H_2O$. In the case of $[AO(CH_2)_6OH]I$, strongly stacked dimers (3.5 Å) are observed, which interact weakly with adjacent dimers. In contrast, the acridine orange rings are infinitely stacked at 3.5 Å in the $[Pt\{AO(CH_2)_6en\}(ox)](NO_3)\cdot 7H_2O$ lattice, and this arrangement is apparently promoted by strong dimeric stacking (3.6 Å) of the nearly planar $\{Pt(en)(ox)\}$ units. This strong hydrophobic stacking may account for the low aqueous solubility of the oxalato derivative, relative to the dichloro or diaqua compounds.

DNA-Binding Studies. Figure 3 displays spectral changes that occur when $[Pt\{AO(CH_2)_6en\}Cl_2]Cl$ (**9**) and $[Pt\{AO(CH_2)_3en\}Cl_2]Cl$ (**20**) are added to calf thymus DNA. Both compounds show a 10–12-nm red shift, together with an increase in the intensity of the 492-nm absorption maximum, upon DNA binding, and both exhibit loss in intensity of the dimer and higher aggregate absorption bands. After 48 h of incubation, further spectral changes occur accompanying the slower, covalent binding of platinum to DNA. For **9**, the position of the monomer absorption maximum shifts by 1 nm, to 506 nm, and the absorbance at the maximum increases slightly, concomitant with a decrease in absorbance at the dimer shoulder. The A_{506}:$A_{478.5}$ ratio increases from 2.20 to 2.32. A sample of similar concentration, in which **9** was bound to calf thymus DNA and then separated from unreacted $[Pt\{AO(CH_2)_6en\}Cl_2]Cl$, gave λ_{max} = 506 nm and A_{506}:$A_{478.5}$ = 2.30 (data not shown). Platinum binding to DNA produces more dramatic changes in the absorption spectrum of **20**. The shoulder at 448 nm due to higher order aggregation disappears, and absorption intensity is transferred to the dimer absorption band at 480 nm and, even more so, to the monomer absorption band at 507 nm (A_{507}:A_{480} increases from 1.79 to 2.14). The position of the band maximum of the DNA adduct of **20** does not shift upon platinum binding, as does that of the **9** adduct, however.

Acridines characteristically exhibit a red shift in their visible absorption maxima upon binding to DNA.[52] After covalent attachment of the platinum moieties of **9** and **20** to DNA, the absorption maxima of the AO moieties remain red-shifted, relative to the free compounds. The shifts are very similar to those of $[AO(CH_2)_6(en)]Cl$, $[AO(CH_2)_3(en)]Cl$, and AO upon binding to DNA (data not shown). This result indicates that the acridine orange rings of all five molecules intercalate into DNA and that intercalative interaction of the acridine orange moieties of **9** and **20** persists even after the platinum is covalently bound to the nucleic acid. Visible absorption data alone, however, cannot reveal whether there has been a redistribution of the equilibrium between intercalated and externally bound AO moieties of **9** and **20** after platinum binding, since visible absorption spectral changes caused by these two DNA-binding modes are similar.[51] Titrations of superhelical DNA are more useful for evaluating the intercalation phenomenon (vide infra).

Visible absorption spectroscopy, however, is useful for assessing intercalator–intercalator interactions. Significant differences occur between the absorption spectra of both **9** and **20** when first added to DNA and following the slower, covalent binding of platinum. In both instances, absorption bands due to dimers and larger aggregates diminish in intensity, while bands due to intercalated monomers grow in intensity. Anchoring the AO moiety to DNA through the covalent platinum linkage decreases self-association of the AO rings. This result suggests that the compounds distribute along the DNA rather than binding in clusters.

We reported previously that $[Pt\{AO(CH_2)_6en\}Cl_2]Cl$ (**9**) unwinds supercoiled pBR322 DNA to the coalescence point with nicked circles at approximately one bound Pt per helical turn, whereas two $[Pt(en)Cl_2]$ molecules are required to cause the same degree of unwinding.[21,53] The enhanced unwinding of DNA by **9** suggests that the AO moiety is intercalatively bound. Some cationic molecules, steroidal diamines in particular, cause unwinding of supercoiled DNA even though they do not intercalate.[54] Flexible cationic molecules such as spermine, however, do not unwind supercoiled DNA.[55] Since **9**, although cationic, has a flexible linker chain, the supercoiled unwinding results are best interpreted by a model in which the AO moiety of **9** intercalates when the platinum moiety is bound to DNA.

Concluding Remarks

A synthetic route has been devised for linking the antitumor complex (1,2-diaminoethane)dichloroplatinum(II) covalently to the DNA intercalator acridine orange by a variable-length polymethylene chain. The syntheses can be carried out on a multigram scale and, for $[Pt\{AO(CH_2)_6en\}Cl_2]Cl$, the overall yield of 32%, based on acridine orange, in the eight-step reaction is good. Visible absorption spectroscopic studies of this compound bound to DNA, together with previously reported DNA superhelix unwinding experiments and exonuclease III mapping studies,[8] establish that the intercalator-linked platinum molecules bind independently to DNA and that the acridine orange moiety of $[Pt\{AO(CH_2)_6en\}Cl_2]Cl$ is able to intercalate one or two base pairs away.

The synergism observed when *cis*-DDP and intercalative drugs are used in combination chemotherapy for the treatment of cancer[5] was in part an incentive for designing and synthesizing the present compounds that incorporate both functionalities into a single molecule. The biological activity[53] of $[Pt\{AO(CH_2)_6en\}Cl_2]Cl$ (**9**) has been examined in mice with L1210 and P388 leukemia and M5076 reticulum cell sarcoma tumor implants to evaluate the potency of this new class of compounds as anticancer agents. The increased life span (% ILS) resulting from treatment with **9** in these screens is significant, although slightly less in general than observed for treatment with *cis*-DDP. Compound **9** is very slightly active against *cis*-DDP-resistant murine tumor implants that show no response to treatment with *cis*-DDP. The strategy employed in the present study for linking platinum to DNA-intercalating molecules suggests possibilities for preparing new compounds for studying anticancer platinum drug binding to DNA and could

(52) Blake, A.; Peacocke, A. R. *Biopolymers* **1968**, *6*, 1225–1253.

(53) Bowler, B. E., Ph.D. Dissertation, Massachusetts Institute of Technology, 1986.

(54) Waring, M. J.; Henley, S. M. *Nucleic Acids Res.* **1975**, *2*, 567–586.

(55) Waring, M. *J. Mol. Biol.* **1970**, *54*, 247–279.

ultimately lead to clinically more effective antitumor drugs.

Acknowledgment. This work was supported by U.S. Public Health Service Grant CA 34992 from the National Cancer Institute. We thank the Engelhard Corp. for a loan of K_2PtCl_4, from which all platinum complexes were prepared. W.I.S. is grateful to the Whitaker Health Sciences Fund for a predoctoral fellowship. B.E.B. acknowledges the Canadian Natural Sciences and Engineering Research Council for a postgraduate scholarship. FAB mass spectra were obtained with the assistance of Dr. C. Costello at the facility supported by NIH Grant RR 00317 (Principal Investigator, Prof. K. Biemann) from the Biotechnology Resources Branch, Division of Research Resources.

Supplementary Material Available: Details of the synthesis of ligands and their precursors, tables reporting final hydrogen and non-hydrogen atom positional and thermal parameters and interatomic distances and angles, and figures showing the structures of **5** and **15** and the stereoviews of $[AO(CH_2)_6OH]I$ and $[AO(CH_2)_3OH]I$ (32 pages); tables of observed and calculated structure factors for **5**, **10**, and **15** (55 pages). Ordering information is given on any current masthead page.

Synthesis and Spectroscopic and X-ray Structural Characterization of Compounds Involving Boron–Phosphorus Multiple Bonds: Lithium Salts of Boryl Phosphides and Their Precursors

Ruth A. Bartlett, H. V. Rasika Dias, Xudong Feng, and Philip P. Power*

Contribution from the Department of Chemistry, University of California, Davis, California 95616. *Received June 27, 1988*

Abstract: The synthesis and spectroscopic and structural characterization of several lithium salts of boryl phosphides and their precursors are described. Treatment of the lithium salt of a primary phosphane H_2PR' with R_2BX (X = F, Cl) affords the phosphinoboranes (borylphosphanes) R_2BPHR' (R/R' = Ph/*t*-Bu (**1**), Mes/*t*-Bu (**2**), Trip/*t*-Bu (**3**), Mes/Ph (**4**), Mes/Cy (**5**), Mes/Mes (**6**) (Mes = 2,4,6-$Me_3C_6H_2$, Trip = 2,4,6-*i*-$Pr_3C_6H_2$, Cy = cyclohexyl)) in good yield. The reaction of compounds **1–6** with 1 equiv of *n*-BuLi or *t*-BuLi affords their corresponding lithium salts $[Li(Et_2O)_2PR'BR_2]$ (**7–12**). The addition of 2 equiv of 12-crown-4 to $Li(Et_2O)_2PR'BMes_2$ (R' = Ph (**10**), Cy (**11**), Mes (**12**)) gives the solvent-separated salts $[Li(12\text{-crown-}4)_2][PR'BMes_2]\cdot THF$ (R' = Ph (**13**), Cy (**14**), Mes (**15**)). Also, the reaction of Mes_2BF with $[Li(THF)_2P(SiMe_3)_2]_2$ gives $[Li(THF)_3P(SiMe_3)BMes_2]$ (**16**) with elimination of Me_3SiF rather than LiF. In addition, the reaction between $TripBBr_2$ and 2 equiv of LiPHMes gave the lithium salt $[Li(Et_2O)_2P(Mes)B(PMesH)Trip]$ (**17**), involving boron bound to two phosphorus centers through a single and a multiple bond. Apart from ^{11}B and ^{31}P NMR spectroscopic characterization, the X-ray structures of the dimeric compound **1**, the lithium salts $[Li(Et_2O)_2P(t\text{-Bu})BTrip_2]$ (**9**), $[Li(THF)_3P(SiMe_3)BMes_2]$ (**16**), and $[Li(Et_2O)_2P(Mes)B(PHMes)\ Trip]$ (**17**) are described. Compounds **10–12** and **13–15**, including the structures of **11**, **12**, and **15**, have been described in a preliminary communication. The lithium compounds **7–17** are of particular interest because they are the only structurally characterized compounds known to involve a high degree of multiple bonding between boron and phosphorus. Thus, compound **17** is also notable since it has the shortest B–P bond length, 1.810 (3) Å, reported to date. Crystal data with Mo Kα radiation (λ = 0.71069 Å) at 130 K: **1**, a = 10.291 (4) Å, b = 10.468 (3) Å, c = 14.767 (2) Å, α = 71.05 (2)°, β = 75.63 (2)°, γ = 82.49 (3)°, triclinic, space group $P\bar{1}$, Z = 2, R = 0.049; **9**, a = 10.378 (4) Å, b = 19.094 (6) Å, c = 21.995 (7) Å, orthorhombic $Pc2_1n$, Z = 4, R = 0.036; **16**, a = 10.331 (6) Å, b = 16.133 (5) Å, c = 10.647 (5) Å, β = 95.13 (4°), monoclinic, space group $P2_1$, Z = 2, R = 0.049; **17**, a = 13.543 (2) Å, b = 17.812 (3) Å, c = 17.475 (3) Å, β = 93.72 (1)°, monoclinic, space group $P2_1/n$, Z = 4, R = 0.063.

Lithium derivatives of the amide (NR_2) and phosphide (PR_2) ligands are the most important transfer agents for these species, and this has generated considerable interest in their structures. Usually they associate in the solid state to form oligomeric or polymeric species involving the nitrogen or phosphorus centers bridging two or more metals. However, the bridging tendency can be reduced by increasing the size of the substitutents on nitrogen or phosphorus. For example, when crystallized from Et_2O or THF, both $LiPPh_2$[1] and $LiP(C_6H_{11})_2$[1] have polymeric chain-like structures whereas $LiP(t\text{-Bu})_2$ is tetrameric[2] and $LiP\{CH(SiMe_3)_2\}_2$ exists as a dimer,[3] even in the absence of donor solvents. In both $LiPR_2$ compounds and their nitrogen counterparts there is a lone pair available on either phosphorus or nitrogen which facilitates their association. It seemed reasonable to assume that if the avilability of the lone pair were to be reduced by electronic rather than steric means, monomeric species might ensue owing to the lower tendency toward bridging. Recent work in this laboratory has shown that, for amide ligands, replacement of one of the alkyl or aryl substituents by the dimesitylboryl group ($BMes_2$) results in amide ligands that have little or no tendency to bridge or behave as π-donors.[4] The use of amide ligands such as $NRBMes_2$ (R = Ph or Mes) has allowed the facile synthesis of a range (d^4–d^8) of two-coordinate transition-metal complexes, for example, $M(NMesBMes_2)_2$ (M = Cr, Mn, Fe, Co, Ni).[5] In addition, the lithium salts $Li(Et_2O)_2NRBMes_2$ (R = Ph, Mes) are monomeric[4,5] even though bulky amide ligands are normally found to be as-

(1) Bartlett, R. A.; Olmstead, M. M.; Power, P. P. *Inorg. Chem.* **1986**, *25*, 1243.
(2) Jones, R. A.; Stuart, A. L.; Wright, T. C. *J. Am. Chem. Soc.* **1983**, *105*, 7459.
(3) Hitchcock, P. B.; Lappert, M. F.; Power, P. P., Smith, S. J. *J. Chem. Soc., Chem. Commun.* **1984**, 1669.
(4) Bartlett, R. A.; Feng, X.; Olmstead, M. M.; Power, P. P.; Weese, K. J. *J. Am. Chem. Soc.* **1987**, *109*, 4851.
(5) Bartlett, R. A.; Chen, H.; Power, P. P. *Angew. Chem., Int. Ed. Engl.*, in press. Power, P. P. *Comments Inorg. Chem.* **1988**, *8*, 177.

0002-7863/89/1511-1306$01.50/0